

# Symmetrical Location Characteristics of Corticospinal Tract Associated With Hand Movement in the Human Brain

## *A Probabilistic Diffusion Tensor Tractography*

*Dong-Hoon Lee, PhD, Do-Wan Lee, PhD, and Bong-Soo Han, PhD*

**Abstract:** The purpose of this study is to elucidate the symmetrical characteristics of corticospinal tract (CST) related with hand movement in bilateral hemispheres using probabilistic fiber tracking method.

Seventeen subjects were participated in this study. Fiber tracking was performed with 2 regions of interest, hand activated functional magnetic resonance imaging (fMRI) results and pontomedullary junction in each cerebral hemisphere. Each subject's extracted fiber tract was normalized with a brain template. To measure the symmetrical distributions of the CST related with hand movement, the laterality and anteriority indices were defined in upper corona radiata (CR), lower CR, and posterior limb of internal capsule.

The measured laterality and anteriority indices between the hemispheres in each different brain location showed no significant differences with  $P < 0.05$ . There were significant differences in the measured indices among 3 different brain locations in each cerebral hemisphere with  $P < 0.001$ . Our results clearly showed that the hand CST had symmetric structures in bilateral hemispheres.

The probabilistic fiber tracking with fMRI approach demonstrated that the hand CST can be successfully extracted regardless of crossing fiber problem. Our analytical approaches and results seem to be helpful for providing the database of CST somatotopy to neurologists and clinical researchers.

(*Medicine* 95(15):e3317)

**Abbreviations:** CR = corona radiata, CST = corticospinal tract, DSI = diffusion spectrum imaging, DTI = diffusion tensor imaging, DTT = diffusion tensor tractography, EEG = electroencephalogram, EPI = echo planar imaging, FL = fiber location, fMRI = functional magnetic resonance imaging, HARDI = high angular resolution diffusion imaging, MAL = most anterior line, MCL = most central line, MLL = most lateral line, MNI = Montreal Neurological Institute, MPL = most posterior line, PLIC =

posterior limb of internal capsule, ROI = region of interest, SAR = specific absorption rate, SLF = superior longitudinal fasciculus.

## INTRODUCTION

The neural fiber tracts in the human brain related with motor movements of hands and feet are the corticospinal tracts (CST), which consists of a group of white matter fibers. They can be separated by the fiber pathways of motor impulse transmission for each motor movement from different cortex areas. Due to its important role in the brain, the assessments of neuroanatomical characteristics for CST are important research topics in surgical planning and management for patients with brain injuries.<sup>1-3</sup> Recently, many studies have attempted to evaluate the neuroanatomical characteristics of the CST pathway using diffusion tensor tractography (DTT), which is derived from diffusion tensor imaging (DTI).<sup>4-14</sup> These researches well performed with their own analytical approaches such as fiber tracking algorithms (deterministic or probabilistic), region of interest (ROI) setting for fiber extraction (user-dependent selection or functional imaging-based selection), and different neuroanatomical measurement methods that were profit to their research proposes. Although many previous results were provided to define the exact neuroanatomical information and some of results were highly correlated with each other, their results still have been remained controversial. Based on the methods and results in the previous literatures, the accurate CST extraction in the human brain should be approached by using the probabilistic fiber tracking algorithm and the functional activation area of specific motor movement.<sup>8,9,13,14</sup> The use of probabilistic fiber tracking algorithm, which is different from the deterministic algorithm, can solve the crossing fiber problem in the brain. The CST is well known fiber that has the fiber crossing regions with superior longitudinal fasciculus (SLF). In addition, the ROI selection process for CST extraction generally depends on the experiences of the researchers. The functional magnetic resonance imaging (fMRI) activation results, which are highly correlated with the specific motor movement tasks at the motor cortex regions, provide accurate ROI selection with consistency in the fiber tracking process to maintain the objectivity of ROI selection.

Therefore, in this study, we attempted to elucidate the symmetrical characteristics of the CST for hand fibers in both hemispheres using DTT combined fMRI and probabilistic fiber tracking algorithm that can provide relatively accurate analysis results. In particular, among several regions in the brain where the CST is passing, we considered 2 brain regions such as corona radiata (CR) and posterior limb of internal capsule (PLIC). These are considered as important locations, because they are commonly affected by stroke and traumatic brain injury resulting poor motor outcome. Note that studying and evaluating more specific characteristics of the CST would be important

Editor: Michael Masoomi.

Received: December 24, 2015; revised: March 9, 2016; accepted: March 14, 2016.

From the Division of MR Research, Department of Radiology, Johns Hopkins University School of Medicine (D-HL, D-WL), Baltimore, MD and Department of Radiological Science, College of Health Science (B-SH), Yonsei University, Wonju, Republic of Korea.

Correspondence: Bong-Soo Han, Department of Radiological Science, College of Health Science, Yonsei University, 1 Yonseidae-gil, Wonju, Gangwon-do 220-710, Republic of Korea (e-mail: bshan@yonsei.ac.kr).

D-HL and D-WL contributed equally to this work.

The authors have no funding and conflicts of interest to disclose.

Copyright © 2016 Wolters Kluwer Health, Inc. All rights reserved.

This is an open access article distributed under the Creative Commons Attribution-NonCommercial-NoDerivatives License 4.0, where it is permissible to download, share and reproduce the work in any medium, provided it is properly cited. The work cannot be changed in any way or used commercially.

ISSN: 0025-7974

DOI: 10.1097/MD.0000000000003317

works for managing the patients or setting the preoperative surgical plans. Therefore, in terms of these perspectives, the investigation of the symmetric distribution of the CST can be also provided a kind of neuroanatomical information and neurological database.

## METHODS

### Subjects and Data Acquisition

Seventeen right-handed healthy subjects (men: 11, age range:  $39.8 \pm 5.6$  years) were participated in this study. They had no previous history of neurological or physical disease. All subjects were provided written informed consent, and the institutional review board of a university hospital approved the study.

DTI and fMRI data were acquired with a 1.5 T MRI system (Gyrosan Intera, Philips Healthcare, Best, The Netherlands) by using a 6-channel phased array brain coil. Both data were obtained with a single-shot spin-echo echo planar imaging (EPI) pulse sequence with following parameters; DTI data (acquisition matrix size =  $96 \times 96$ , reconstruction matrix size =  $128 \times 128$ , field of view [FOV] = 221 mm, time of repetition [TR]/time of echo [TE] = 10,726/76 ms, sensitivity encoding [SENSE] factor = 2, b-value =  $1000 \text{ s/mm}^2$ , 32 noncollinear diffusion-sensitizing gradients, slice thickness = 2.3 mm, and 67 contiguous transverse slices with no gap), and fMRI data (matrix size =  $64 \times 64$ , FOV = 210 mm, TR/TE = 2000/60 ms, slice thickness = 5 mm, SENSE factor = 2, 26 contiguous transverse slices with no gap, and a block paradigm [right-hand grasp-release movements at 1-Hz frequency for task (Rest/Activation time = 21/21 s, repeated 3 times)]). The interleaved acquisition method was applied to reduce the cross-talk effect between slices.

### Data Analysis

fMRI data were analyzed using SPM5 (Department of Cognitive Neurology, London, UK) software with uncorrected  $P < 0.05$ . A 8-mm full width at half maximum sized Gaussian kernel was applied to all fMRI data to increase the validity of statistics.<sup>8,15</sup> The fMRI data were realigned and co-registered based on the nondiffusion weighted image (b=0 image) because the analyzed fMRI activation results, which were spatially registered to b=0 image, were used for the ROI setting in the fiber tracking process.

DTI data were analyzed using FSL ([www.fmrib.ox.ac.uk/fsl](http://www.fmrib.ox.ac.uk/fsl), Analysis Group, FMRIB, Oxford, UK) software which processed by a probabilistic tractography method based on multifiber model. Before the data analysis, eddy current distortion correction process was performed using a tool named as "Eddy current correction" on the FSL software. For the eddy current correction, each subject's diffusion-weighted volume images were aligned to b=0 image (reference volume) using 12 parameters affine registration. For the CST fiber tracking in each cerebral hemisphere, 2 ROIs were determined with hand movement-related fMRI activation area including the precentral knob in the cortex region for seed ROI selection and pontomedullary junction of the CST (blue portion of the anterior pontomedullary junction) area in the color-coded V1 image for target ROI selection.<sup>12</sup> Fiber tracking process was performed with following criteria: 5000 streamline, 0.5 mm step length, and 0.2 curvature thresholds, where the extracted fibers were generated by passing through the 2 sets of ROIs simultaneously.<sup>16</sup> After fiber tracking, the b=0 image from each

subject was normalized to the Montreal Neurological Institute (MNI) EPI template, and then the transformation matrix were acquired. Using this transformation matrix, extracted CST volume images in each hemisphere were also normalized to MNI EPI template.

### Measurement of CST Symmetrical Characteristics

Measurements of CST symmetrical distribution were performed with the locations of extracted fiber in the upper CR, lower CR, and PLIC of bilateral hemispheres. The measurement processes were divided into 2 indices such as laterality index and anteriority index on the normalized brain (Figure 1). Based on the normalized brain, the laterality index was defined as a distance ratio between the connected line from the most central line (MCL) that separates the brain to both hemispheres to the most lateral line (MLL) and the connected line from the MCL to fiber location (FL) point. The anteriority index was defined as a distance ratio between the connected line from the most anterior line (MAL) to the most posterior line (MPL) and the connected line from the MAL to FL point. In all measurement processes, the laterality index and anteriority index were measured in the upper/lower CR location that are defined by the transverse locations where we can observe the minimal/maximum size of lateral ventricle, and in the PLIC location that is defined by the transverse location where we can observe the level of the insular cortex. In addition, the FL was determined by the location of the highest pixel value in the extracted fibers in each transverse plane, which are in upper CR, lower CR, or PLIC. The highest pixel value represents the highest probabilistic location of fiber tract.<sup>12</sup>

### Statistical Analysis

For statistical analysis, SPSS software (v.17.0; SPSS, Chicago, IL) was used. A paired *t* test was used for the values of laterality index and anteriority index between the right and left hemispheres. In addition, the statistical analysis among 3 different brain locations in each cerebral hemisphere was performed by 1-way ANOVA, followed by Tukey post hoc test. The significant level of the *P* value was set at 0.05 in all statistical analysis processes.

## RESULTS

The measured laterality index and anteriority index for right-hand and left-hand fibers were represented in Figure 2 and Table 1. In the PLIC, measured laterality index values were  $22.36 \pm 1.28$  (right) and  $22.06 \pm 1.27$  (left), and anteriority index values were  $91.39 \pm 1.92$  (right) and  $92.07 \pm 1.78$  (left). Based on the statistical results using paired *t* test, no significant differences were observed between right and left hemispheres of laterality and anteriority indices ( $P = 0.59$ , laterality index;  $P = 0.34$ , anteriority index). In the lower CR and upper CR, measured laterality index values were  $23.92 \pm 1.24$  (right, lower CR),  $23.69 \pm 1.09$  (left, lower CR),  $25.57 \pm 0.88$  (right, upper CR), and  $25.03 \pm 1.01$  (left, upper CR), and anteriority index values were  $87.01 \pm 2.02$  (right, lower CR),  $86.89 \pm 1.81$  (left, lower CR),  $85.71 \pm 1.47$  (right, upper CR), and  $86.03 \pm 1.77$  (left, upper CR). In these results, there were also no significant differences between right-side measured indices and left-side measured indices (laterality indices,  $P = 0.59$  at lower CR and  $P = 0.08$  at upper CR; anteriority indices,  $P = 0.85$  at lower CR and  $P = 0.52$  at upper CR). However, in the ANOVA statistical

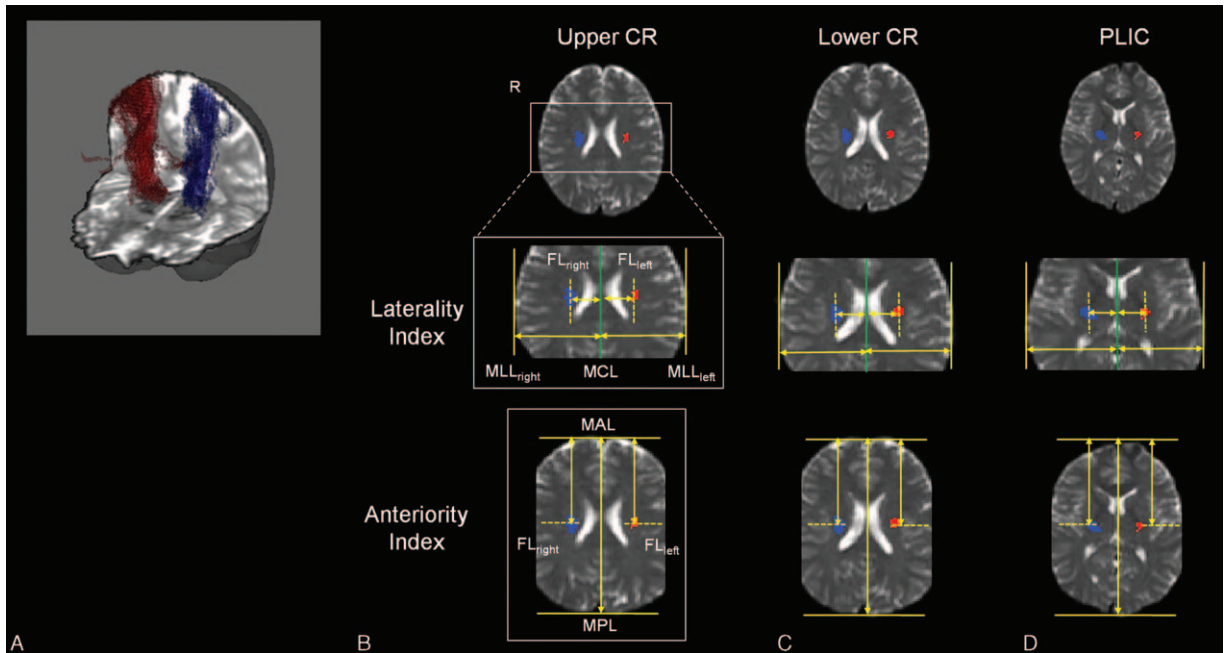


**FIGURE 1.** Measurement procedures of laterality index and anteriority index at upper CR (B), lower CR (C), and PLIC (D) for a representative subject (blue/red: fiber tract in each cerebral hemisphere). (A) The DTI tracking results of CST related with hand movement in bilateral hemispheres for a representative subject. The baseline image was normalized  $b = 0$  image with MNI EPI template. CR = corona radiata, CST = corticospinal tract, DTI = diffusion tensor imaging, EPI = echo planar imaging, FL = fiber location, MAL = most anterior line, MCL = most central line, MLL = most lateral line, MNI = Montreal Neurological Institute, MPL = most posterior line, PLIC = posterior limb of internal capsule.

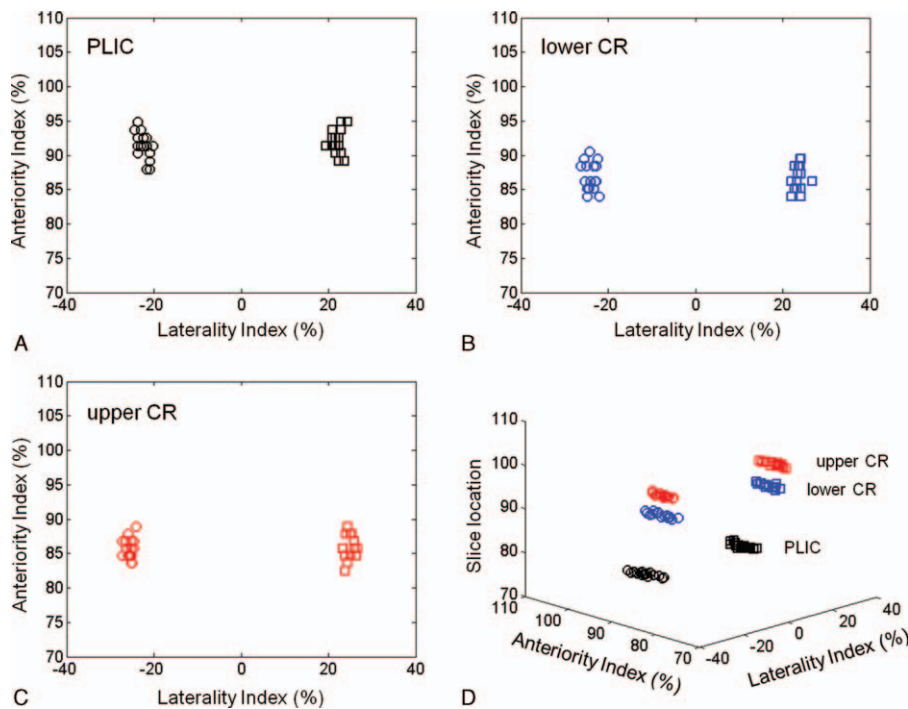


**FIGURE 2.** Measured values for laterality index and anteriority index at PLIC (A), lower CR (B), and upper CR (C) from each subject. (D) The overall distributions of measured values in 3-dimensional coordinates, which represented the slice locations according to each brain location. CR = corona radiata, PLIC = posterior limb of internal capsule.

**TABLE 1.** Measured Values of the Laterality Index and Anteriority Index of the CST Related With Hand Movement in the PLIC, Lower CR, and Upper CR

	PLIC		Lower CR		Upper CR	
	Right	Left	Right	Left	Right	Left
Laterality index, %	22.36 ± 1.28	22.06 ± 1.27	23.92 ± 1.24	23.69 ± 1.09	25.57 ± 0.88	25.03 ± 1.01
Anteriority index, %	91.39 ± 1.92	92.07 ± 1.78	87.01 ± 2.02	86.89 ± 1.81	85.71 ± 1.47	86.03 ± 1.77

All values represented mean ± standard deviation.

CR = corona radiata, CST = corticospinal tract, PLIC = posterior limb of internal capsule.

analysis results among 3 different brain locations in each cerebral hemisphere, there were significant differences were found in all values from each other ( $P < 0.001$ ), except the anteriority values between lower CR and upper CR at right hemisphere ( $P = 0.10$ ) and at left hemisphere ( $P = 0.35$ ).

## DISCUSSION

Evaluation and investigation of neuroanatomical characteristics on in vivo CST possess important meanings in brain researches due to the direct relationship between the CST and many types of motor movements. Many studies have been indicated the neuroanatomical information of the CST using various analytical approaches such as DTT, electroencephalogram, or invasive intraoperative neurosurgery.<sup>17–21</sup> Especially, the DTT can clearly visualize in vivo neural fiber tract without any invasive approaches. Based on the DTT method, various studies have been performed to verify the characteristics of the CST including FLs, somatotopic arrangements between motor fibers, and differences in between normal subjects or patients.<sup>2,8–10,12,22,23</sup> However, the results from previous studies of CST somatotopy indicated some controversial issues and discrepancies due to the differences in approach and the accuracy of the analysis. In addition, interestingly, there are only few studies on finding symmetries of CST, and it is not dealt as an important issue in the research areas using DTT method although providing the symmetrical information of CST was a branch of somatotopy research considering its clinical importance for neurosurgery or neurorehabilitation. Based on the results from previous studies inferred symmetric characteristics of CST somatotopy, Hong et al<sup>12</sup> showed the CST somatotopic locations at pons, which is also an important pathway for CST in 2010. Although they did not directly evaluated the symmetrical information of CST at pons, it can be deduced using the measured information of the somatotopic location. Their results indicated 2 findings. First, the CST for hands was located in the anteromedial portion of the pons compared with the CST for leg location. Second, based on their measured values, the symmetrical distribution of CST had no significance at the pons. In a different study, Pan et al<sup>9</sup> showed the results on the somatotopic organization of CST at PLIC in 2012. Their results demonstrated that the somatotopic arrangement of bilateral hemispheres was in symmetric distribution at PLIC. These studies still remained some limitations since there were absences of fMRI combination with fiber tracking and/or small numbers of diffusion gradient orientation.

In this study, we evaluated symmetrical distribution information of the CST related with hand movement in bilateral hemispheres while we complemented the shortcomings of previous studies. We acquired DTI data with 32 gradient

orientations, and fiber tracking process was performed with multifiber probabilistic tractography algorithm to avoid the crossing fiber problems between the CST and the SLF. In addition, fMRI activation results were used to set ROI in motor cortex region, and brain normalization method was used to maintain the objectivity of symmetrical information of the CST. Our results indicated that the hand CST had negligible differences of symmetrical distribution. Notably, these symmetrical distributions also had no significant differences even when the brain location was changed. These are also clearly represented in the statistical analysis results that were calculated by paired *t* test in 3 different locations. On the other hand, the statistical analysis results that were calculated by ANOVA among 3 brain locations in each cerebral hemisphere showed significant differences. These were considered as the result due to the characteristics of anatomical location of the hand CST, which originates from the cerebral motor cortex to pons, in the brain. The CST has not only a straight-forward direction, but also showed a little curved shape in the superior–inferior direction, and the anterior–posterior direction in the brain. Therefore, in between the brain locations, the relatively measured laterality indices and anteriority indices may represent the significance. However, interestingly, our ANOVA statistical results on anteriority indices of hand CST between upper CR and lower CR showed no significant differences in each cerebral hemisphere unlike the other ANOVA statistical results. In other words, they represent the anteriority indices between 2 locations have similar anatomical location distributions, and they seem to be affected by the measurement process of the anteriority index. Similar to our study, in previous studies, they also measured the anteriority distance index of hand CST in the CR brain level using the ratio based on the distance between anterior and posterior pole of the lateral ventricle. They also found that the anteriority distances for hand CST between upper CR and lower CR have some differences although they did not provide the statistical analysis results.<sup>8,24</sup> However, in our anteriority index measurement process, we defined the basis distance for the ratio using whole brain length, which is measured from the distance between the most anterior and the most posterior point of the normalized brain template structures in the CR brain level. Therefore, our results should be different from those of previous studies, and our measurement processes may also affect the statistical analysis results, although we measured the anteriority indices in a similar way to the previous studies.

As the DTI data acquisition strategies and analytical techniques have developed, the accuracy of the results has also improved. The DTI data acquisitions with high angular resolution diffusion imaging (HARDI) method or diffusion spectrum imaging (DSI) method are introduced to be able to solve the crossing fiber problems and to extract more information from

the diffusion signal.<sup>25–27</sup> Unlike general DTI method, the HARDI method is measuring the diffusion signal using a lot of uniformly distributed diffusion gradient directions (>50) than required for DTI, and it can be extracted high angular frequency features of the diffusion signal. Moreover, the DSI also measures the signal in many different directions; however, it uses a lot of diffusion gradient strengths unlike the HARDI method. Although these newly developed methods have advantages for the improvement of result accuracy, relatively long scan times (>30 min) and high specific absorption rates on in vivo can be disadvantages in clinical applications. While many techniques are being developed to solve these problems gradually, there is still unknown that become clinically popularized by general DTI method because of the other clinical limitations. In contrast, the postprocessing algorithms, which are to solve the crossing fiber problem and to increase the accuracy of results, have been widely used due to the ease of use and accessibility. Representative method is a probabilistic fiber tractography algorithm, which uses the information calculated from a spatial distribution of a streamline in a single seed voxel rather than a single tract.<sup>14,28</sup> This processing approach can provide more accurate information of complex fiber structures such as a crossing fiber area. Although the probabilistic fiber tracking algorithm have a limitation on the time consumption due to its computational time in multiorientation of each voxel, it has been solved by using multiple parallel computing calculation process in recent years.

This study has limitation point that considered CST related with hand movement from various movements-related CSTs such as foot, face, and tongue in the human brain. By using fiber tracts related with multiple movements, it should be able to provide more detailed symmetrical characteristics of CST in the human brain. These approaches will be investigated in a future study.

## CONCLUSIONS

Investigation of somatotopic organizations of hand movement-related CST including symmetrical information or location distribution in the human brain is able to provide the helpful information to neurologist and neuroscientist who clinically studied about neuroradiological anatomy or surgical planning of brain diseases. In particular, to the best of our knowledge, there are not many researches for symmetrical characteristics of CST. We believe that our analytical approaches for fiber tracking and present results seem to be useful datasets for clinical applications.

## REFERENCES

1. Wang L, Yu C, Chen H, et al. Dynamic functional reorganization of the motor execution network after stroke. *Brain*. 2010;133:1224–1238.
2. Yeo SS, Jang SH, Son SM. The different maturation of the corticospinal tract and corticoreticular pathway in normal brain development: diffusion tensor imaging study. *Front Hum Neurosci*. 2014;8:573.
3. Schaechter JD, Fricker ZP, Perdue KL, et al. Microstructural status of ipsilesional and contralesional corticospinal tract correlates with motor skill in chronic stroke patients. *Hum Brain Mapp*. 2009;30:3461–3474.
4. Mori S, Crain BJ, Chacko VP, et al. Three-dimensional tracking of axonal projections in the brain by magnetic resonance imaging. *Ann Neurol*. 1999;42:265–269.
5. Xue R, van Zijl PC, Crain BJ, et al. In vivo three-dimensional reconstruction of rat brain axonal projections by diffusion tensor imaging. *Magn Reson Med*. 1999;42:1123–1127.
6. Melhem ER, Mori S, Mukundan G, et al. Diffusion tensor MR imaging of the brain and white matter tractography. *Am J Roentgenol*. 1999;178:3–16.
7. Yamada K, Kizu O, Mori S, et al. Brain fiber tracking with clinically feasible diffusion-tensor MR imaging: initial experience. *Radiology*. 2003;227:295–301.
8. Lee DH, Hong C, Han BS. Diffusion-tensor magnetic resonance imaging for hand and foot fibers location at the corona radiata: comparison with two lesion studies. *Front Hum Neurosci*. 2014;8:752.
9. Pan C, Peck KK, Young RJ, et al. Somatotopic organization of motor pathways in the internal capsule: a probabilistic diffusion tractography study. *Am J Neuroradiol*. 2012;33:1274–1280.
10. Seo JP, Chang PH, Jang SH. Anatomical location of the corticospinal tract according to somatotopies in the centrum semiovale. *Neurosci Lett*. 2012;523:111–114.
11. Conti A, Raffa G, Granata F, et al. Navigated transcranial magnetic stimulation for “somatotopic” tractography of the corticospinal tract. *Neurosurgery*. 2014;10(Suppl 4):542–554.
12. Hong JH, Son SM, Jang SH. Somatotopic location of corticospinal tract at pons in human brain: a diffusion tensor tractography study. *Neuroimage*. 2010;51:952–955.
13. Koch G, Bozzali M, Bonni S, et al. fMRI resting slow fluctuations correlate with the activity of fast cortico-cortical physiological connections. *PLoS ONE*. 2012;7:e52660.
14. Parker GJ, Haroon HA, Wheeler-Kingshott CA. A framework for a streamline-based probabilistic index of connectivity (PICO) using a structural interpretation of MRI diffusion measurements. *J Magn Reson Imaging*. 2003;18:242–254.
15. Guo Y, Pagnoni G. A unified framework for group independent component analysis for multi-subject fMRI data. *Neuroimage*. 2008;42:1078–1093.
16. Smith SM, Jenkinson M, Woolrich MW, et al. Advances in functional and structural MR image analysis and implementation as FSL. *Neuroimage*. 2004;23:S208–S219.
17. Ostrý S, Belšan T, Otáhal J, et al. Is intraoperative diffusion tensor imaging at 3.0T comparable to subcortical corticospinal tract mapping? *Neurosurgery*. 2013;73:797–807.
18. Simon MV, Cole AJ, Chang EC, et al. An intraoperative multimodal neurophysiologic approach to successful resection of precentral gyrus epileptogenic lesions. *Epilepsia*. 2012;53:e75–e79.
19. Wu G, Wang L, Liu J, et al. Minimally invasive procedures reduced the damages to motor function in patients with thalamic hematoma: observed by motor evoked potential and diffusion tensor imaging. *J Stroke Cerebrovasc Dis*. 2013;22:232–240.
20. Wu J, Quinlan EB, Dodakian L, et al. Connectivity measures are robust biomarkers of cortical function and plasticity after stroke. *Brain*. 2015;138:2359–2369.
21. Yasokawa YT, Shinoda J, Okumura A, et al. Correlation between diffusion-tensor magnetic resonance imaging and motor-evoked potential in chronic severe diffuse axonal injury. *J Neurotrauma*. 2007;24:163–173.
22. Holodny AI, Gor DM, Watts R, et al. Diffusion-tensor MR tractography of somatotopic organization of corticospinal tracts in the internal capsule: initial anatomic results in contradistinction to prior reports. *Radiology*. 2005;234:649–653.
23. Weiss C, Tursunova I, Neuschmelting V, et al. Improved nTMS- and DTI-derived CST tractography through anatomical ROI seeding on anterior pontine level compared to internal capsule. *Neuroimage Clin*. 2015;7:424–437.
24. Kim JS, Pope A. Somatotopically located motor fibers in the corona radiata: evidence from subcortical small infarcts. *Neurology*. 2005;64:1438–1440.

25. Tuch DS, Reese TG, Wiegell MR, et al. High angular resolution diffusion imaging reveals intravoxel white matter fiber heterogeneity. *Magn Reson Med.* 2002;48:577–582.
26. Wedeen VJ, Hagmann P, Tseng WI, et al. Mapping complex tissue architecture with diffusion spectrum magnetic resonance imaging. *Magn Reson Med.* 2005;54:1377–1386.
27. Berman JI, Lanza MR, Blaskey L, et al. High angular resolution diffusion imaging probabilistic tractography of the auditory radiation. *Am J Neuroradiol.* 2013;34:1573–1578.
28. Behrens TE, Berg HJ, Jbabdi S, et al. Probabilistic diffusion tractography with multiple fibre orientations: what can we gain? *Neuroimage.* 2007;34:144–155.